which must meet the appropriate performance criterion (e.g., 10,000 pW0p). This adjustment to the system noise budget results in a further modification to the previously calculated system parameters. For example, the INTELSAT V system has been designed to meet a 10,000 pW0p criterion (Gray and Brown-1979). The composite received downlink must meet 7500 pW0p, with the remaining 2500 allocated to terrestrial and intersystem interference. This 7500 pW0p corresponds to a C/N of about 14 dB, yet the composite downlink thermal noise C/N is about 5 to 8 dB larger than this value, to allow for intermodulation products and for frequency reuse interference.

We do not consider here the employment of adaptive techniques to cancel cross-polarized components and to enable systems to operate at high levels of depolarization (e.g., 10 dB). By using such techniques, one pushes the outage threshold level of depolarization back to a value which effectively "never" occurs, so that the outages stem from attenuation alone.

7.3.6.3 Apply Lesser Propagation Effects. Attenuation effects from other than precipitation generally are of "second order" for system design purposes. Indeed, they may not need to be considered in the first iteration. They will be needed, however, for later, more accurate, estimates of performance.

"Clear air" attenuation, in excess of free space path loss, will typically be less than one or two dB except at the shortest millimeter wavelengths (greater than 50 GHz) or near absorption bands. These values may be calculated as shown in Figure 6.2-3. Adjustments are then made to the nominal performance power budgets (previously computed on a free-space-loss basis).

Cloud, fog, and dust attenuation factors may be very difficult to incorporate unless adequate statistics for their occurrence are available. These phenomena have significant effect only in unusual system designs, because the amount of attenuation is generally much less than that of rain. In general, a system with a fair amount of

rain margin will also have sufficient margin to operate through clouds. In addition, clouds and fog are not likely to occur so often as to influence the nominal performance value (50 or 80% of the time). Where appropriate, however, the system designer may incorporate an additional margin to allow for these attenuation effects. Similarly, signal fluctuations and antenna gain degradations, as treated in Paragraph 6.5, are relatively small and need be considered only in later iterations of performance analysis, at which time the effect can be accounted for through small margin adjustments to the nominal path loss.

7.3.6.4 Adjust System Parameters and Analyze System Performance. In the foregoing, adjustment of system parameters has been carried out simultaneously with the development of the examples. The system designer may choose to use this approach, or to defer these adjustments until this point in the process. To do this in an organized manner, one should accumulate all propagation impairments which are (or can be equated to) attenuations or losses into a composite margin. Increases in sky noise, and the interference components, can be equated to losses in signal power, as previously discussed. This composite margin will be offset by power or gain adjustments. These margins and consequent system parameter adjustments are applied to the nominal system performance budget. In the analog example, this was the 10,000 pW0p criterion. Separately, the more severe effects which cannot be offset by (reasonable) margin are treated according to an outage criterion, i.e., by addition of outages contributed by each. Adjustments to system parameters resulting from a deficiency in meeting this criterion often involve fundamental changes in qualitative system design rather than simply margin changes. As an example, if the outage time is excessive because the system concept is very sensitive to mild depolarization, it may be necessary to use a different type of polarization, adaptive polarization techniques, or a different modulation technique.

In order to illustrate this step of the design process using the examples, a recapitulation of the constraints and parameters determined up to this point is in order. This is done in Table 7.3-2 for the digital system, and in Table 7.3-3 for the analog system.

The parameters for the digital system example from Table 7.3-2 are now used to carry out a detailed link power budget analysis, shown in Table 7.3-4. Here the power budget equation is applied to determine the C/N on the uplink and downlink separately. The individual C/N values are then combined to give the composite C/N. This is done for both the clear air or nominal case and the degraded case. The clear air budget includes an allowance of 0.5 dB for clear air attenuation (estimated using the data of Section 6.2.2), antenna pointing error, and other minor degradations. The degraded budget includes the rain attenuation exceeded for 0.5% of the time, as estimated earlier, and the increase in ground terminal noise temperature that is expected during the 0.5% downlink rain. This "sky noise" contribution was neglected earlier.

The nominal composite C/N for the digital system clearly exceeds the minimum required for at least 80% of the time (10.7 dB). When rain attenuation and sky noise have been included, however, the composite C/N is 0.4 dB less than the required value for 99% of the time (9.0 dB). We note that this deficiency can be easily made up by increasing the uplink transmitted power to 40W (16dBW), shown in parentheses in the Table 7.3-4 budget table.

The corresponding power budget calculations are carried out for the analog example in Table 7.3-5. In this case, the nominal composite C/N exceeds the minimum by nearly 4 dB, and the degraded value is 0.8 dB better than required. The 4 dB "overkill" under nominal conditions suggests that uplink power control would be advisable in this case to decrease the disparity in power level between the nominal and faded carriers in a transponder's passband.

Table 7.3-2. Digital System Summary

Specified Performance Criteria	Bit Error Rate $\leq 10^{-6}$ $\geq$80% of the time $\leq 10^{-4}$ $\geq$99% of the time (outage time $\leq$1%)
Modulation and Performance	Data Rate: 40 Mb/s Modulation: QPSK Coding: Rate 1/2, Convolutional Required C/N (in symbol rate bandwidth) BER = 10^{-4} : 9.0 dB BER = 10^{-6} : 10.7 dB
System Parameters	14 GHz uplink, 12 GHz downlink TDMA (no power sharing or intermodulation in satellite repeater)
Satellite Parameters	EIRP = 43 dBW G/T = 3 dB
Ground Terminal Parameters	Receive noise temperature = 300K Receive antenna gain = 53.7 dBi Transmit antenna gain = 55 dBi Transmitted power = 15.2 dBW

Table 7.3-3. Analog System Summary

Specified Performance Criteria	≤10,000 pW0p ≥80% of the time ≤100,000 pW0p ≥99.7% of the time "Outage" exists when 500,000 pW0p is reached
Modulation and Performance	120 channel FDM-FM trunks pW0p C/kT 10,000 84.1 100,000 74.1 500,000 67.1
System Parameters	30 GHz uplinks, 20 GHz downlinks Dual (site) diversity, up- and downlinks Number of trunks per transponder: 8 Transponder channel bandwidth: 40 MHz
Satellite Parameters	Antenna transmit gain: 36 dBi Receive G/T: 3 dB Transmit power total (with backoff): 3 dBW per carrier: -6 dBW
Ground Terminal Parameters	Receive noise temperature: 200 K Receive antenna gain: 63 dBi Transmit antenna gain: 66.5 dBi Transmitted power (per carrier): 20 dBW

Table 7.3-4. Digital Example Power Budgets

	Uplink (14GHz)	Downlink (12GHz)
Transmit Power (dBW)	15.2 (16)*	
Antenna Gain (dBi)	55	
EIRP (dBW)	70.2	43
Free Space Loss (dB)	-206.4	-205.1
G/T (dBK^{-1})	3	28.9
Boltzmann's Constant (dB)	-(-228.6)	-(-228.6)
Clear Air and Other Propagation Losses (dB)	-0.5	-0.5
Nominal Link C/kT(dB-Hz)	94.9 (95.7)*	94.9
Reference Bandwidth, 80MHz (dBHz)	79	79
Nominal Link C/N (dB)	15.9 (16.7)*	15.9
Nominal Composite C/N (dB)	12.9 (13.3)*	
Rain Attenuation, ≤0.5% of Time (dB)	-4	-2.9
Sky Noise Increase, 134K (dB)		-1.6
Degraded Link C/N (dB)	11.9 (12.7)*	11.4
Degraded Composite C/N, ≤1% of Time (dB)	8.6 (9.0)*	

* 40 Watt transmit power case

Table 7.3-5. Analog Example Power Budgets

	Uplink (30GHz)		Downlink (20GHz)
Transmit Power (dBW)	20		-6
Antenna Gain (dBi)	66.5		36
Free Space Loss (dB)	-213		-209.5
G/T (dBK^{-1})	3		40
Boltzmann's Constant (dB)	-(-228.6)		-(-228.6)
Clear Air and Other Propagation Losses (dB)	-1.5		-1.2
Nominal Link C/kT (dB-Hz)	103.6		87.9
Nominal Composite C/kT (dB-Hz)		87.8	
Rain Attenuation, ≤0.15% of Time (dB)	-38.2		-17.2
Diversity Gain	+13		+10
Sky Noise Increase, 220K (dB)			-3.2
Degraded Link C/kT (dB-Hz)	78.4		77.5
Degraded Composite C/kT, ≤0.3% of Time (dB-Hz)		74.9	

The power budget shown for the analog system does not include some noise contributions that should be considered in the next iteration of the design. Those contributions include self-interference, interference from other satellite and terrestrial systems, and intermodulation in the satellite repeater. Self-interference may arise from crosstalk between frequency bands, orthogonal polarizations, antenna patterns, or combinations of the three, as determined by the system architecture.

7.3.6.5 Iterate System Design and Analysis. This phase needs little explanation. If the initial design does not, per analysis,deliver the level of performance required, the design must be changed in some way. Various trade-off techniques may be used to assist the design engineer in deciding what to change. The next section describes some of these techniques. In some cases, a critical look at the system requirements themselves must be taken. The examples that have been presented here were simplified in several respects, so that the several modifications to initial design assumptions could be made as the design proceeded. In an actual, real-world design, more refined analyses and iterations would be needed. Both of the examples used a particular terminal rain rate and elevation angle assumption. For a real system with a distribution of terminals in various locations, considerable refinement of the approaches would be possible, and could have significant impact in reduction of power requirements and/or outage times. Also, the examples did not illustrate the consideration of criteria other than long term (outage percentage) statistics.

7.3.7 Supplementary Design Tools

Techniques are available for assigning rain margins and allocating link performance parameters with more precision than has been used in the examples. We describe two of them here and provide references to others.

The first technique incorporates rain attenuation, sky noise temperature increase due to rain, and satellite repeater non-linearity into the carrier-to-noise trade-off relation given earlier. The composite carrier-to-noise ratio (C/N)c on a satellite circuit with rain effects is given by the formula

$$(C/N)_C = \left[(C/N)_U^{-1} L_U^{-1} + (C/N)_D^{-1} L_D^{-1} n(L_D) b^{-1}(L_U)\right]^{-1} \qquad (7.3\text{-}6)$$

where

$(C/N)_U$ = clear air value of uplink carrier-to-noise ratio

L_U = uplink rain attenuation

$(C/N)_D$ = clear air value of downlink carrier-to-noise ratio

$n(L_D)$ = downlink noise power increase factor due to sky noise temperature

$b(L_U)$ = satellite repeater output power reduction factor due to decrease in input power

All the parameters in the formula are expressed as numerical values, rather than decibels. The factor $n(L_D)$ is the fractional increase in noise temperature (and therefore downlink noise power) corresponding to the downlink rain attenuation L_D. For example, by the formulas in Section 6.7.4, the increase in antenna noise temperature accompanying a rain producing a 5 dB fade is about 188K (assuming surface temperature = 290K). If the ground terminal clear sky noise temperature was 300K, then the temperature increase factor n(5dB) would be 488/300 = 1.6 (2.1 dB). The factor $b(L_u)$ is a function of the nominal operating point and the characteristics of the satellite repeater (typically a TWT operating near saturation). If the fractional output power reduction corresponding to an input power reduction (uplink loss, L_U) of 5 dB were 3 dB, then b(5dB) = 0.5.

Figure 7.3-5 shows the trade-off curve defined by the equation for three conditions. (All parameters are shown in decibels for convenience.) Curve A corresponds to the clear-air condition and is the same as Figure 7.3-2. For curve B we assume uplink rain only. It is curve A shifted up by the factor $b(L_U)$ (in decibels) and to the right by the uplink attenuation L_U. Curve C assumes downlink rain only, and it is curve A shifted up by the downlink rain attenuation L_D plus the noise temperature increase factor n(LD) (in decibels). If L_U is the uplink attenuation exceeded for P_D % of the time, then curve B gives the corresponding values of $(C/N)_U$ and $(C/N)_D$ that will achieve at least the required $(C/N)_C$ except for P_U % of the time, assuming no downlink rain. Likewise if L_D is the downlink attenuation exceeded P_D % of the time, then curve C gives the corresponding C/N combinations assuming no uplink rain. The intersection of the two shifted curves B and C is the combination of C/N values that gives at least the required composite $(C/N)_C$ except for $P_U + P_D$ % of the time, assuming uplink and downlink rain do not occur simultaneously. Since the probability of jointly determined outages is much less than that of uplink or downlink outages (see Section 7.3.5.1), this technique gives a good approximation to the values of $(C/N)_U$ and $(C/N)_D$ needed to achieve the required outage time percentage $P_U + P_D$. The method requires an initial allocation of outage time to the uplink and downlink. To optimize system parameters, it could be carried out for a range of allocations.

This technique, since it does not consider carrier suppression, interference, or intermodulation noise, is most applicable to single carrier operation as in TDMA systems. The method is discussed by Calo, et. al. (1978) who carry out the computation of optimum uplink and downlink system parameters for a 12/14 GHz TDMA system. It is also used by McGregor (1981) in an example system design.

The second method of analysis to be described was used by Kittiver and Westwood (1976) in supporting the satellite-ground system design of the Satellite Business Systems network. This method, termed the Composite Margin Plane (CMP) analysis, permits a

precise calculation of link availability (or alternately, outage time percentage) given the rain attenuation statistics for the uplink and downlink and the system performance parameters. The CMP analysis is based on the equation for composite carrier-to-noise ratio given earlier, but takes the uplink and downlink rain attenuations as the independent variables. Satellite repeater non-linearity and downlink sky noise are not considered explicitly, but may be allowed for. The equation for $(C/N)_C$, disregarding these terms, can be plotted on the L -L coordinates as shown in Figure 7.3-6. The region contained within the curve represents the combination of uplink and downlink attenuation values that will result in a composite carrier-to-noise ratio less than $(C/N)_C$, taken as the outage value. The CMP plot is dependent on the clear-air values of $(C/N)_U$, $(C/N)_D$, and $(C/N)_C$ assigned, so requires an allocation of these parameters at the outset. Its utility lies in the fact that the independent variables coincide with those of the measured (or predicted) attenuation statistics. To determine circuit availability (1-outage probability) we must calculate the integral

$$P_{avail} = \int\int Pxy\ (x,\ y)\ dxdy \qquad (7.3\text{-}7)$$

$$(C/N)_C > \min\ (C/N)_C \qquad (7.3\text{-}8)$$

where

P_{avail} = availability

X = uplink attenuation

Y - downlink attenuation

p_{XY} = Joint probability density function of X, Y

The CMP defines the boundary of the region of the X-Y plane over which the integral is carried out. On the boundary the "composite" rain margin is zero. Outside the boundary the margin is negative

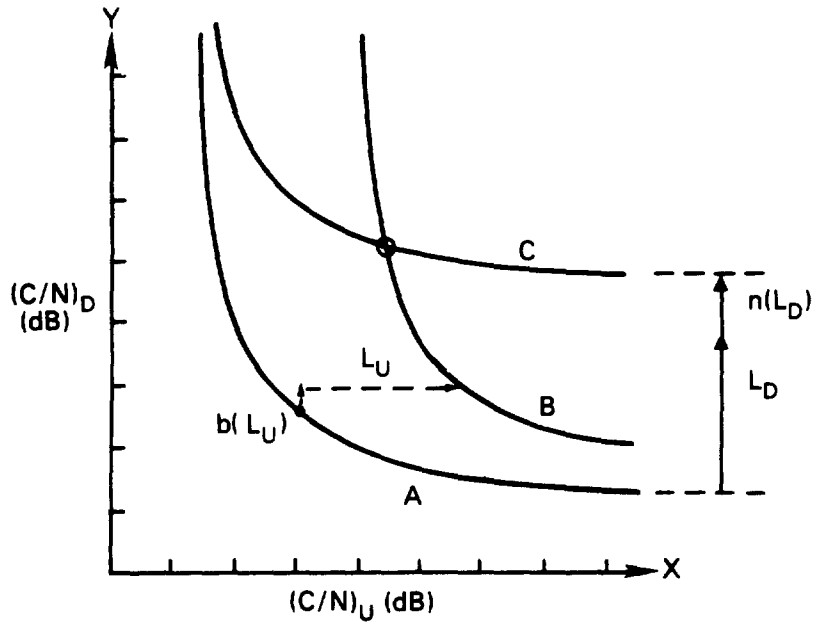

Figure 7.3-5. Uplink and Downlink Carrier to Noise Ratio Tradeoff

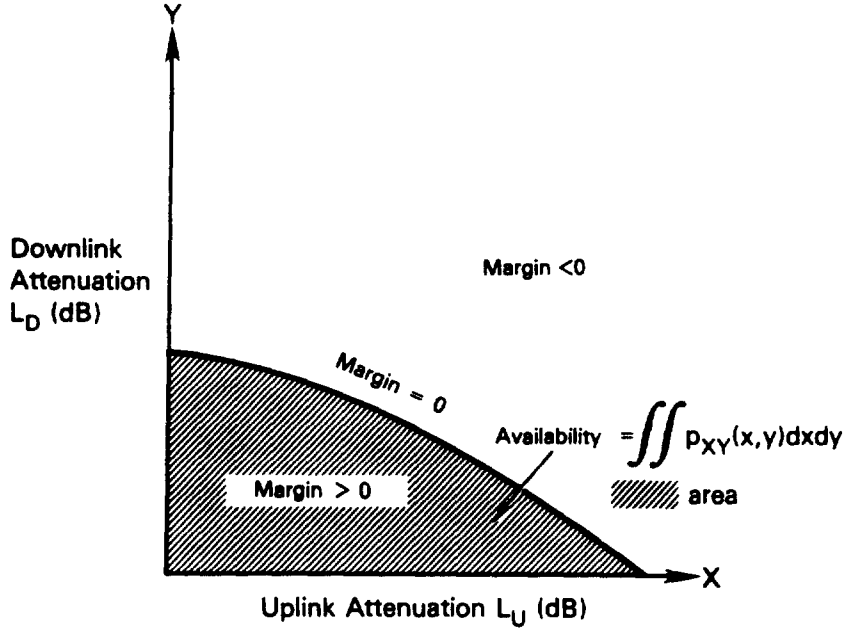

Figure 7.3-6. Composite Margin Plane

or the circuit is unavailable. The probability density function p_{XY} is given by the product of the uplink and downlink probability density functions (pdf's), which are in turn determined from the attenuation exceedance statistics plots for the uplink and downlink ground terminal locations. Since the joint pdf is taken as the product of the individual pdf's, we are implicitly assuming that the uplink and downlink attenuations are statistically independent, which is usually a reasonable assumption.

Kittiver and Westwood (1976) carried out the availability calculation by this method for 12/14 GHz circuit between Washington, D.C. and Atlanta, Georgia. The steps are illustrated in Figure 7.3-7, reproduced from the referenced paper. The CMP is shown in part (a) for the selected clear air values of $(C/N)_U$ and $(C/N)_D$. The dotted lines indicate that the C/N on each link is considered to be reduced by an implementation margin of 1.5 dB. The CMP, adjusted by this margin, is again modified by the downlink sky noise contribution. Part (b) shows the effect of downlink sky noise as an equivalent increase in downlink attenuation. Using part (b) to revise the ordinate of the CMP yields part (c). Part (d) shows the attenuation exceedance statistics measured for the up- and downlink locations at the respective frequencies. This is used to label the axes of the CMP with the exceedance percentages, as shown in part (e). Using the data in part (e), it is possible to graphically integrate the joint pdf and arrive at a value for the availability. Further details are given in the references.

A simplification of the CMP graphical integration is used by Calo, et. al. (1976) and McGregor (1981). The simplification consists of finding the sum of the integrals over two regions of the CMP, $L_U > L_{UMAX}$ and $L_D > L_{DMAX}$, as indicated in Figure 7.3-8. The approximate value of availability obtained in this way does not include the integral over the region bounded by the zero margin line and the L_{UMAX}, L_{DMAX} rectangle, but includes twice the integral over $L_U > L_{UMAX}$, $L_D > L_{DMAX}$. The unavailability (1-availability) given by this is equal to the probability that uplink rain reduces the margin

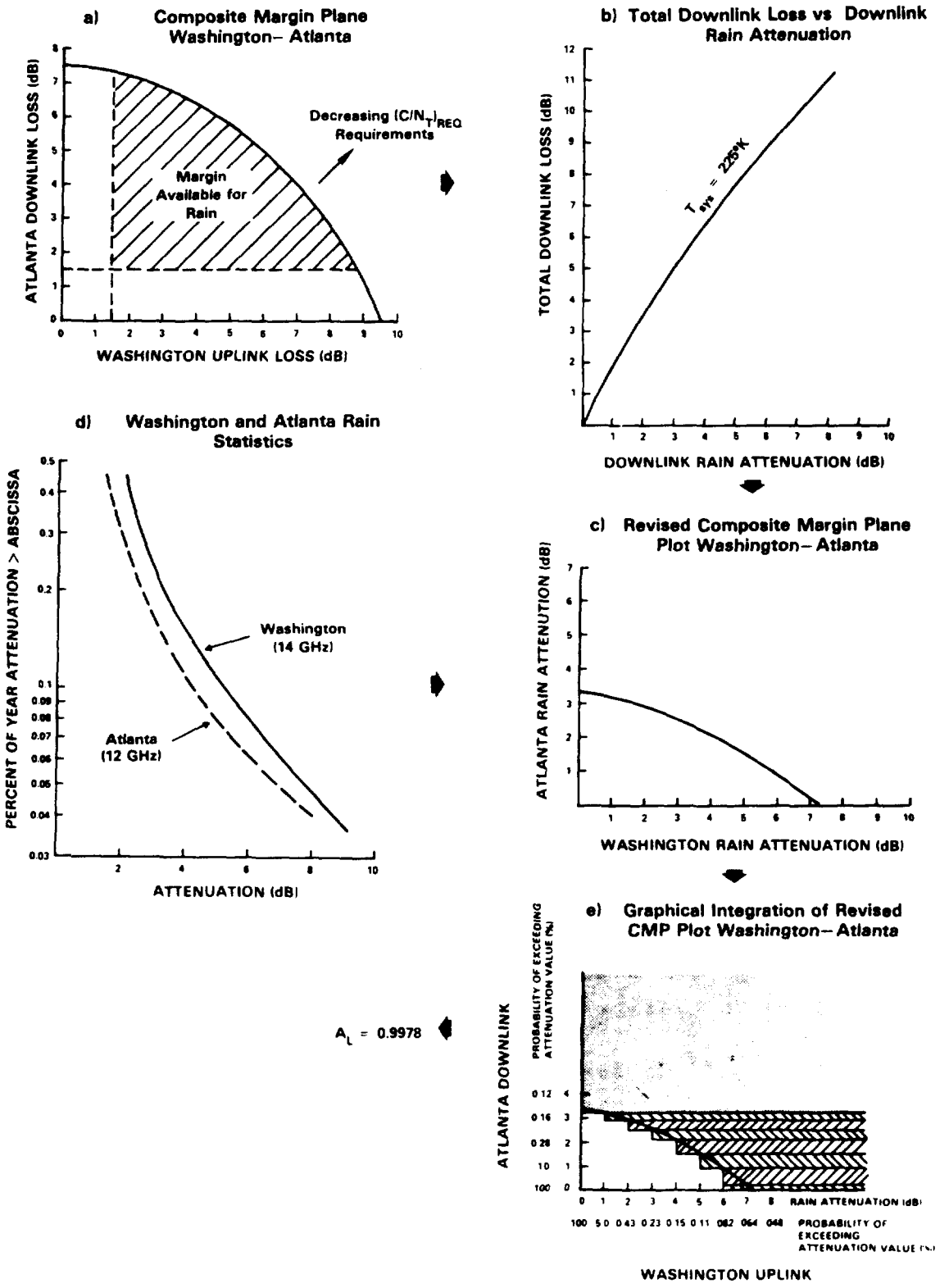

Figure 7.3-7. Composite Margin Plane Availability Analysis (from Kittiver - 1976)

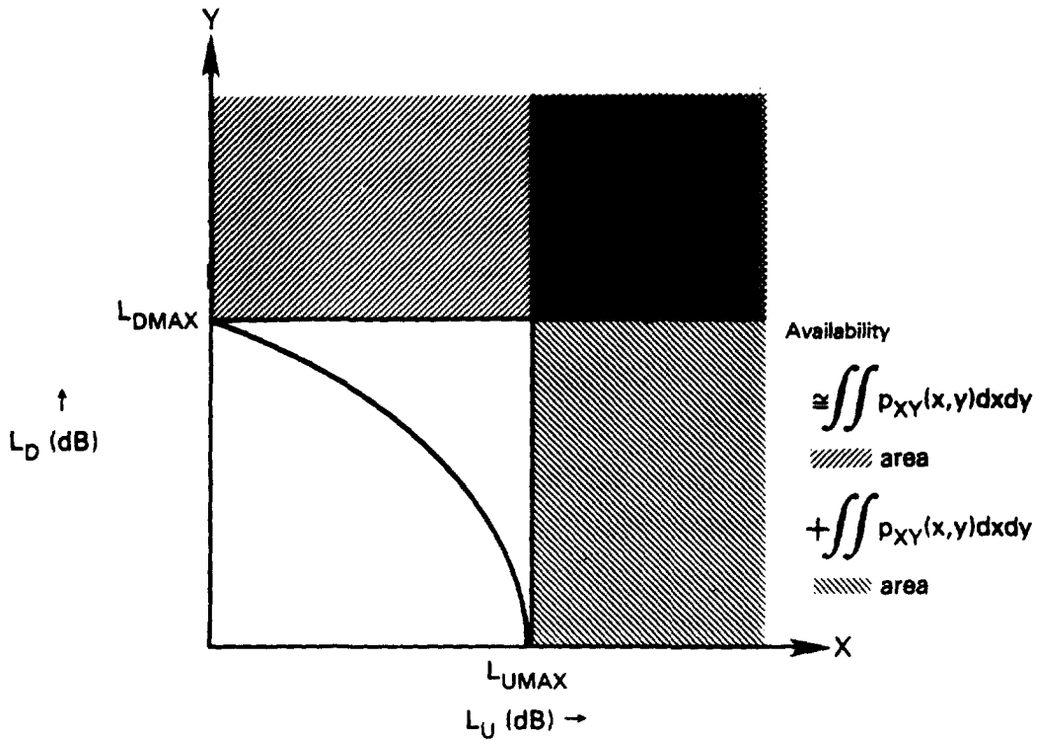

Figure 7.3-8. Approximate Composite Margin Plane Analysis

to zero with no downlink rain, or, that the downlink rain reduces the margin to zero with no uplink rain. Thus the approximation is the same as that used in the C/N trade-off analysis of Figure 7.3-4.

Other techniques for calculating system availability have been described in the literature. Lyons (1974, 1976) has performed statistical availability analyses including the effects of repeater non-linearity and limiting, intermodulation noise, and uplink power control in FDMA systems. Bantin and Lyons (1978) studied the effects of rain, scintillation, ground terminal antenna pointing error, and satellite station-keeping on system availability statistics. Because they require complex computer evaluation, the techniques described in these papers are not easily applied. Also,

their use is limited to one or two multiple access configurations. McGregor (1981) presents a method of finding system availability that is general in its approach and does not require computer evaluation. The method allows one to find the pdf of the composite carrier-to-noise ratio for a satellite circuit, considering the characteristics of the multiple access configuration, the propagation effects statistics, and the statistical characteristics of the body of users accessing the satellite. In the referenced report, the method is applied to the availability analysis of a code-division (spread-spectrum) multiple access system.

7.4 RAIN FADE MITIGATION

There are, of course, several brute-force methods that can be used to combat rain attenuation. One method is simply to operate at as low a carrier frequency as possible. However, for reasons already discussed, satellite communication is going to higher rather than lower frequencies. Another method of combatting rain attenuation is to increase either the transmitter EIRP or the receiver G/T, or both, in order to improve the performance margin. However, because of technological, regulatory, and radio interference considerations, one can go only so far in raising system EIRPs and G/Ts to improve performance margins. In fact, rain attenuation statistics presented in Chapter 3 of this Handbook indicate that highly reliable satellite communication systems operating in the millimeter-wave bands above 20 GHz would need excessive power margins to mitigate rain fades. So other, more clever, means for mitigating rain fades are clearly needed for good system performance.

With a view toward commercial utilization of the 20/30 GHz satellite bands, researchers are investigating techniques for dealing with the problem in elegant and cost-effective ways. Much of this work (Bronstein - 1982) is sponsored by NASA as part of the Advanced Communication Technology Satellite (ACTS) program, which

has the goal of making the 20/30 GHz bands technologically accessible to U.S. industry (NASA - 1987).

The amount of rain attenuation is, of course, extremely time and space sensitive. For example, in many densely populated areas on the eastern seaboard of the United States, propagation impairments due to rain are especially acute because of the timing of thunderstorm activity. Thunderstorms occur predominately during the peak in communication traffic between the east and west coasts. Nevertheless, one can overcome this extreme spatial sensitivity by using various space diversity techniques to combat rain fades. Space diversity involves the use of two or more spatially separated links for redundancy. If, at some instant, one of the redundant links experiences a fade, a spatially separated link may not experience a fade at the same instant. So we can switch to the link that provides the better performance. Careful timing of link switchovers can overcome the time sensitivity of rain fades. Examples of appropriate space diversity techniques for combatting rain fades are:

1. Site diversity (multiple transmitting and/or receiving terminals), and

2. Orbit diversity (multiple satellites).

In a similar vein, one can combat rain fades either by adaptively adjusting certain signal parameters to existing propagation conditions, or by using redundant signals. For example, a link experiencing a fade at one frequency may not experience fading at another (lower) frequency. So one can switch to a frequency that provides acceptable performance whenever a severe rain fade occurs. Examples of appropriate signalling techniques for combatting rain fades are:

1. Transmitter power control

2. Adaptive forward error correction

3. Frequency diversity

4. Data rate reduction.

In this Handbook these signalling techniques are considered as possible implementations of "signal diversity" schemes.

These and other approaches (Ippolito - 1986, Brandinger - 1978, and Engelbrecht - 1979) have been suggested as techniques for significantly improving communication reliabiilty in the presence of rain attenuation. More experimental results have been obtained for site diversity than for any other form of rain fade mitigation. However, system designers will want to consider combinations of all diversity options. Complexity and cost will play major roles in the ultimate decision to use any diversity technique.

The following sections discuss each of these techniques for rain mitigation.

7.4.1 Measures of Diversity Performance

To characterize the performance of diversity systems, one must establish suitable performance parameters. One such parameter in common use is "diversity gain". Suppose the rain attenuation on a single diversity branch (a single propagation path or a single carrier frequency, for example) is A dB at some instant. The attenuation will vary with time, so let A(T) be the value of A that is exceeded T percent of the time. To obtain good fade statistics (and therefore an accurate estimate of T), we must assume that the attenuation has been measured over a sufficiently long time period. Now suppose additional diversity branches (site diversity or frequency diversity, for example) are introduced to reduce the effective rain attenuation. Let $A_{div}(T)$ be the value of A that is exceeded T percent of the time after diversity has been introduced. As illustrated in Figure 7.4-1, we can define the diversity gain (Hodge - 1974a) to be the difference between A(T) and $A_{div}(T)$ at the value of T that has been selected:

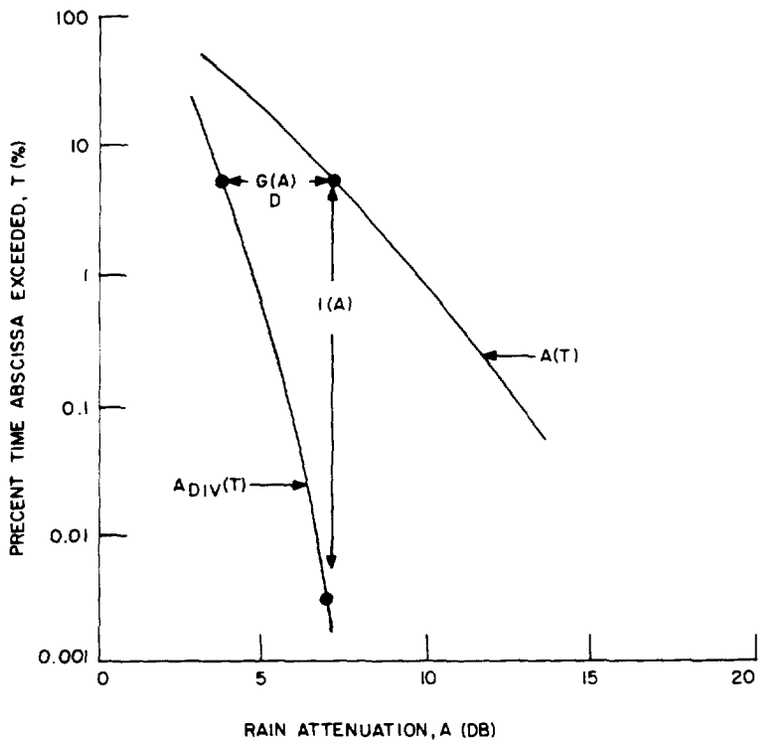

Figure 7.4-1. Definition of Diversity Gain and Advantage

$$G_D(A) = A(T) - A_{div}(T) \qquad (7.4\text{-}1)$$

Another measure of diversity performance is "diversity advantage" (Wilson and Mammel - 1973). Let T(A) be the percentage of time that some attenuation A (in dB) is exceeded when there is no diversity. Similarly, let $T_{div}(A)$ be the corresponding value of T when diversity is employed. As illustrated in Figure 7.4-1, we can define diversity advantage as the ratio of these two quantities at the selected value of A:

$$I(A) = \frac{T(A)}{T_{div}(A)} \qquad (7.4\text{-}2)$$

If the system designer specifies that a given attenuation A (with or without diverstiy) may not be exceeded more than T percent of the time, then the diversity gain turns out to be the reduction in EIRP or G/T that the introduction of diversity permits, while maintaining the specified value of T. On the other hand, suppose instead that the system designer wants to specify the value of the

attenuation above which a rain-induced system outage is considered to occur. Then the diversity advantage is the factor by which the outage duration can be reduced by introducing diversity, while maintaining other system parameters such as EIRP and G/T constant. Clearly, these two parameters (diversity gain and diversity advantage) are not independent descriptors of diversity performance because Figure 7.4-1 shows that when one of the two parameters is known, the other is readily determined.

Up to now we have implicitly assumed that the fade statistics associated with each diversity branch are identical. In practice this is seldom the case. Attenuation statistics differ on the two branches either because of measurement uncertainty or because of real differences that exist among the diversity branches. A quantitative description of this effect would require more than one parameter to characterize diversity performance. But the use of only a single parameter is very convenient, and furthermore there is little reason a priori to assign more weight to one branch than to another. One way to get around this difficulty is to use average values for the single-branch attenuation and time percentage, and to define the diversity gain and diversity advantage as

$$G_D(A) = A_{ave}(T) - A_{div}(T) \qquad (7.4\text{-}3)$$

$$I(A) = \frac{T_{ave}(A)}{T_{div}(A)} \quad , \qquad (7.4\text{-}4)$$

which are simple generalizations of eqs. 7.4-1 and 7.4-2. The averages in eqs. 7.4-3 and 7.4-4 are over the possible diversity branches.

Allnutt (1978) used both diversity gain and diversity advantage to compare diversity data. He showed that the use of diversity gain allows trends and similarities to be readily observed, while the use of diversity advantage with the same data produces results with a large amount of scatter. In explaining these observations, Hodge (1982) pointed out that the use of diversity advantage requires

measurements over widely different time intervals. Uncertainties in the values of $T_{ave}(A)$ and $T_{div}(A)$ being compared are therefore very different, which apparently accounts for the widely fluctuating values. A second drawback to using diversity advantage as a performance parameter is that it often cannot be defined when deep fades occur because the estimate of $T_{div}(A)$ for large A requires excessively long measurement times. These arguments suggest that data analysis and comparison are better done on the basis of diversity gain than diversity advantage. If required, diversity advantage can then be determined later, when the analysis in terms of diversity gain is complete.

7.4.2 Space Diversity

At carrier frequencies exceeding 10 GHz, rain attenuation often degrades earth-space propagation paths so seriously that the requirements of economical design and reliable performance cannot be achieved simultaneously. To overcome this problem, Hogg(1968) proposed the use of site diversity on earth-space paths to achieve the desired level of system reliability at reasonable cost. This proposal was based on the hypothesis that the intense rain cells that cause the most severe fading are rather limited in spatial extent. Furthermore, these rain cells are usually separated from one another, which means that the probability of simultaneous fading on two paths to spatially separated earth terminals is less than that associated with either individual path. Wilson (1970) first tested this hypothesis, using radiometric noise emission measurements to determine the rain attenuation on separated paths. Hodge (1974a) later tested the hypothesis, using actual earth-space paths. These and other enusing experiments have demonstrated that site diversity is an effective technique for improving system reliability in the presence of rain attenuation.

Figure 7.4-2 shows a typical configuration employing site diversity. Also indicated are definitions of the following parameters, which are needed in later discussions:

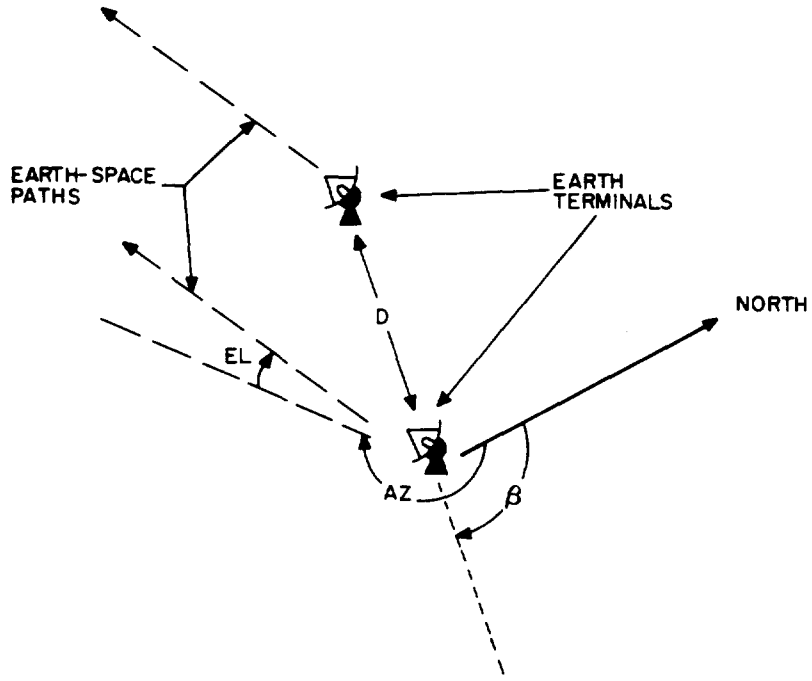

Figure 7.4-2. Site Diversity Configuration

AZ = azimuth of earth-space path (degrees)

EL = elevation of earth-space path (degrees)

d = distance between earth terminals (km)

β = orientation of earth terminal baseline (degrees)

Orbit diversity, on the other hand, uses only one ground site to communicate via two or more earth-space paths with satellites located in separated orbital positions, as illustrated in Figure 7.4-3. If a rain cell is far from the terminal, so that the cell is not likely to intercept more than one path to the terminal, the result will be similar to that for site diversity. However, if a rain cell is near the terminal, little improvement results because

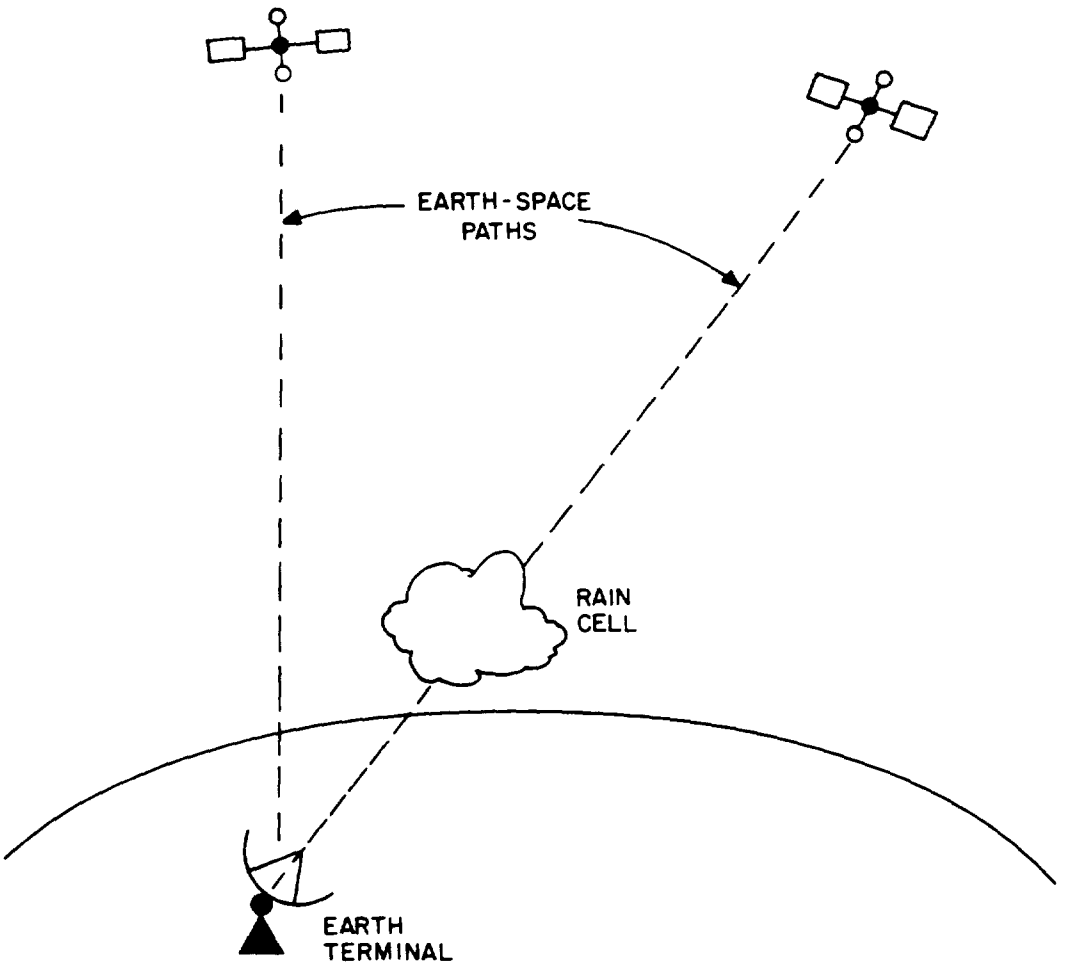

Figure 7.4-3. Orbit Diversity Configuration

all paths to the terminal pass through the same cell. Orbit diversity is therefore not as effective as site diversity in some cases. Nevertheless, in other situations orbit diversity can provide significant rain fade mitigation whenever multiple satellites are available.

7.4.2.1 Site Diversity

The following discussion of site diversity begins with a summary of numerous site diversity experiments that have been performed. Then, after discussing the various design factors that are required to quantitatively describe site diversity, some mathematical models for estimating the diversity gain that is achievable from site diversity are presented. The first model to be discussed is empirical in the sense that measured diversity data are fitted to simple equations in order to obtain formulas for the diversity gain. The second model is analytical in the sense that a definite statistical distribution for the rain attenuation is used to estimate the diversity gain.

7.4.2.1.1 Site Diversity Experiments

Table 7.4-1 presents a list of experimental diversity measurements available in the literature provided by Hodge (1982). [Additional information on diversity measurements can be found in Figures 4 and 5 of Annex I to Report 564-3 of CCIR (1986).] This table includes the results reported for each of the four methods -- direct measurement of satellite beacons, radiometric measurement of the sky temperature, radar measurements of rain structures and radiometric measurements of solar emission. In each case the reference is cited along with the location of the experiment, the frequency, station separation distance, baseline orientation, path azimuth, and path elevation. In cases where multiple measurements are reported, the range of the appropriate parameters is indicated. A fifth method, rapid response raingauges, has been attempted, but has not been accurate for predicting diversity gain. The two reasons cited (Allnutt-1978) are: 1) the rainfall rate on the

Table 7.4-1. Summary of Diversity Experiments

I. SATELLITE EXPERIMENTS

REFERENCE	LOCATION	FREQ.	SEPARATION(d)	BASELINE ORIENTATION (β')	AZ	EL
Hodge (1974)	Columbus, Ohio	15.3 GHz	4.0-8.3 km	159-164°	210°	38°
Westinghouse (1975)†	Washington, DC area	20, 30	27.9-75.8	Several	≈206°	≈40°
Hodge (1976b)	Columbus, Ohio	20, 30	13.2-14.0	33-151°	197°	40°
Vogel, et al (1976)	Austin, Texas	30	11.0	0°	172°	55°
Hyde (1976)	Boston, Mass.	18	6.7-35.2	74-93°	212°	36°
	Columbus, Ohio	18	5.1-38.9	91-95°	196°	42°
	Starkville, Miss.	18	8.3-40.0	105-113°	190°	51°
Hosoya, et al (1980)	Yokohama, Japan	20	19	164°	188°	48°
Suzuki, et al (1982)	Kashima, Japan	20	45	0°	190°	48°
Tang, et al (1982)	Tampa, Florida	19, 29	11, 16, 20	157, 244, 210	198-205°	31°-57°
Towner, et al (1982)	Blacksburg, Va.	11.6	7.3	160°	106°	10.7°

II. RADIOMETER EXPERIMENTS

Wilson (1970)	Crawford Hill, N.J.	16	3.2-14.4	135°	226°	32°
Wilson & Mammel (1973)	Crawford Hill, N.J.	16	11.2-30.4	135°	226°	32°
Gray (1973)	Crawford Hill, N.J.	16	19.0-33.0	45-135°	226°	32°
Funakawa & Otsu (1974)	Kokubunji, Japan	35	15.0	---	180°	45°
Hall & Allnutt (1975)	Slough, England	11.6	1.7-23.6°	20-106°	198°	30°
Allnutt (1975)	Slough, England	11.6	1.7-23.6°	20-106°	198°	30°
Strickland (1977)	Quebec, Canada	13	18.0	11°	122°	19°
	Ontario, Canada	13	21.6	1°	116°	16°
Bergmann (1977)	Atlanta, Georgia	17.8	15.8-46.9	141-146°	228°	38°
	Denver, Colorado	17.8	33.1	86°	197°	43°
Rogers (1981)	Graz-Michelbachberg, Austria	11.4/12	10.9	---	154°	33°
	Etam-Lenox, WV	11.6	35	---	114°	18°
	Kurashiki City - Shimotsui, Japan	12	17	---	260°	6°

III. RADAR EXPERIMENTS

Goldhirsh & Robison (1975)	Wallops Island, Va.	13-18	2-20	0-180°	0-360°	45°
Goldhirsh (1975)	Wallops Island, Va.	13-100	2-20	0-180°	0-360°	45°
Goldhirsh (1976)	Wallops Island, Va.	18	2-20	0-180°	0-360°	45°
Hodge (1978)	Montreal, Quebec	13	4-42	0-180°	122-240°	19-40°

IV. SUNTRACKER EXPERIMENTS

Wulfsburg (1973)	Boston, Mass.	35	11.2	158°	---	---
Funakawa & Otsu (1974)	Kokubunji, Japan	35	15.0	---	---	---
Davies & Croom (1974)	Slough, England	37	10.3	67°	---	---
Davies (1976)	Slough, England	37	10.3-18.0	67-110°	---	---

† Long-Baseline Site Diversity Experiment